




Experimental evaluation of the thermophysical performance of an adaptive composite wall system under dynamic climatic conditions

Zhangabay N.Zh.¹ , Oner A.K.² , Ibrahim M.N.M.³ ,
Ibraimova U.B.¹ , Kolesnikov A.S.¹ , Tursunkululy T. *¹ 

¹ South-Kazakhstan University named after M. Auezov, Kazakhstan,

² Abylkas Saginov Karaganda Technical University, Kazakhstan,

³ Universiti Sains Malaysia, Malaysia

Abstract: In the sharply continental and hot climate of Kazakhstan, improving building energy efficiency requires adaptive composite envelope systems capable of dynamically responding to external thermal loads. This study provides experimental validation of a newly developed adaptive energy-efficient wall assembly with alternating air channels and a radiant barrier, previously proposed and numerically investigated by the authors. The experiments were conducted in a climatic chamber using a full-scale 3×3 m wall fragment under two operating modes: cold conditions (−14.3 °C) and hot conditions (+26.4 °C with exterior cladding heated up to +46 °C). Interlayer temperatures, heat flux density, and thermal bridging in the bracket zone were measured, and both calculated and effective thermal transmittance resistance values were determined in accordance with regulatory requirements. The experimental results demonstrated strong agreement with numerical simulations: deviations in interlayer temperatures did not exceed 3-7%, while heat flux density differed by 6-9%. The wall configuration Scheme 3/50/75/50 exhibited pronounced adaptive behavior; switching to the ventilation mode during the hot period reduced heat flux density by up to 14% and decreased the temperature gradient within the air channel by an average of 3-5 °C. Under cold conditions, the system increased thermal resistance by up to 18% compared with assemblies without a reflective layer. The obtained effective thermal resistance values comply with the building standards of the Republic of Kazakhstan and confirm the energy efficiency of the wall system for operation in extreme climates. Overall, the experimental validation confirms the reliability of the model and the high practical applicability of the adaptive wall technology. The findings provide a scientifically grounded basis for the development of façade design standards optimized for Central Asian climates and demonstrate the potential for implementation in both new construction and retrofit projects.

Keywords: adaptive composite wall system, model validation, thermal resistance, climatic chamber testing, ventilated façade, radiant barrier, life safety

*Corresponding author E-mail: timurtursunkululy@gmail.com

Please cite this article as: Zhangabay N.Zh., Oner A.K., Ibrahim M.N.M., Ibraimova U.B., Kolesnikov A.S., Tursunkululy T. Experimental evaluation of the thermophysical performance of an adaptive composite wall system under dynamic climatic conditions. *Construction Materials and Products*. 2026. 9 (1). 8. DOI: 10.58224/2618-7183-2026-9-1-8

1. INTRODUCTION

Adaptive building envelope systems incorporating air cavities are considered among the most promising solutions for improving building energy efficiency under significant climatic loads. In regions with hot and sharply continental climates, such as southern and central Kazakhstan, envelope structures are exposed to combined effects of high ambient temperatures, intense solar radiation, large diurnal temperature variations, and variable aerodynamic loads. These factors necessitate scientifically grounded design solutions aimed at enhancing the thermal performance of façades and ensuring their durability [1].

Despite the availability of theoretical and numerical studies addressing the behavior of ventilated façades, the scientific literature lacks data obtained under conditions corresponding to extreme radiative loads and high air temperatures [2-4] typical of Kazakhstan's climate [5]. This highlights the need for a comprehensive review of existing research and for dedicated experimental investigations. Ventilated façade systems with air channels have been investigated in a wide range of experimental, theoretical, and numerical studies, confirming their relevance for improving building energy efficiency and enhancing envelope resilience to external climatic loads. Borodulin and Nizovtsev [6-8] model coupled heat and moisture transfer processes in panel façade systems with ventilation channels and identify a significant potential of such structures to reduce thermal loads, improve moisture exchange, and prevent condensation accumulation. Their results emphasize the importance of proper channel-parameter selection to enhance natural ventilation and maintain stable temperature conditions. Experimental studies by Statsenko et al. [9] confirm the effectiveness of ventilated façades under real operating conditions. The study demonstrates that an air cavity contributes to smoothing temperature differences, reduces the amplitude of diurnal temperature fluctuations, and improves the moisture regime of the envelope. The authors also stress the need to account for channel height, wind speed, and cladding material properties, since these parameters significantly influence the intensity of natural convection.

Works [10, 11] examine heat transfer characteristics in multilayer envelope systems and provide a detailed analysis of how airflow velocity and direction depend on channel geometry, surface roughness of materials, and temperature gradients. These findings confirm that even minor modifications of the cavity configuration may substantially affect façade thermal behavior. The study by Yuan [12] highlights the importance of assessing thermal inertia and the decrement factor (attenuation of temperature fluctuations), which determine the ability of envelope structures to store and delay heat transfer. This aspect is particularly relevant for adaptive façade systems in hot climates, where the magnitude of thermal load is governed not only by solar radiation intensity but also by the ability of materials to compensate for short-term temperature peaks.

Optimization of thermal insulation materials is addressed in detail in the studies by Özturan [13], Shahid [14], and Uçar [15], which establish relationships between insulation thickness, regional climatic features, and building energy consumption. These studies indicate that the optimal insulation thickness should be determined with consideration of local climatic conditions, including the number of sunny days, radiative heating levels, and diurnal temperature variations. Aggarwal [16] demonstrates that the performance of thermal insulation materials varies significantly across climate zones. The author shows that in hot climates preference should be given to materials with high solar reflectance and low thermal inertia, whereas in cold regions materials with high heat storage capacity are more effective. This study emphasizes the need for an adaptive approach to envelope design and material selection accounting not only for annual mean temperatures but also for extreme climatic conditions. A comprehensive review of climate-adaptive façade designs with an air cavity is provided by Vasileva et al. [17], with particular attention to the interplay between ventilation channel geometry,

thermophysical properties of materials, and external climatic factors. The authors show that the performance of adaptive façades largely depends on the air-gap configuration, including cavity height, thickness, shape, and the arrangement of inlet and outlet openings. It is also emphasized that using materials with different reflective and absorptive characteristics enables control over the façade thermal regime and improves energy efficiency under variable solar radiation. The study justifies the need for an integrated façade design approach combining aerodynamic modeling, heat-flux analysis, and assessment of dynamic temperature evolution. The review by Cuce and Cuce [18] complements this perspective by considering ventilated façades as a key technology for low-carbon and energy-efficient construction. The authors conclude that such systems provide multifunctional benefits, including reduction of operational energy use, mitigation of thermal loads on load-bearing walls, enhancement of natural ventilation, and improvement of indoor comfort through microclimate stabilization. The review also highlights the role of innovative materials such as nanostructured coatings, photoreflective layers, and materials with variable thermal conductivity capable of adapting to temperature fluctuations and solar loads. Further development of the technology is expected to involve the integration of active adaptive elements and intelligent thermal-flow control systems. The experiment reported by Lin et al. [19] provides evidence of the real behavior of ventilated façades in cold climates and demonstrates the dominance of thermoconvective processes under large temperature differences. The authors record variations in airflow velocity inside the channel, formation of stable and unstable convective cells, and non-uniform temperature distribution as a function of façade-element height. These experimental findings confirm the need to account for spatial and temporal non-uniformities in façade modeling and also indicate that conclusions derived for cold climates cannot be directly transferred to hot climates without appropriate adaptations [20-23]. To analyze envelope durability and resistance to thermomechanical effects, it is recommended to employ studies on fatigue crack propagation in multilayer structures [24-26]. These works show that cyclic thermal loads caused by diurnal temperature variations and periodic solar heating may lead to a gradual degradation of mechanical strength in cladding and structural elements. The studies consider crack initiation and growth mechanisms, the influence of material heterogeneity on service life, and the impact of thermal gradients on local stress states. These findings are particularly relevant for the design of adaptive façade systems, as they allow risk assessment of defect formation, prediction of service life, and justification of additional reinforcing or damping elements.

The conducted literature analysis allows several critical limitations to be identified, which restrict the direct applicability of existing findings to the climatic conditions of Kazakhstan:

- Focus on temperate climates. Studies [6-8, 14-16] consider temperature ranges that are not comparable with extreme heat (+40...+50 °C) and high solar radiation typical for Kazakhstan.
- Limited experimental evidence. Only studies [9] and [16] include full-scale field investigations; however, they do not account for intense solar radiation and cladding heating above +45 °C.
- Lack of data on foil-based reflective layers. The presence of a reflective coating (foil) may significantly alter the solar energy absorption spectrum, yet this aspect remains largely unexplored.
- Insufficient durability and defect formation data. Studies [24-26] highlight the importance of assessing thermocyclic stresses; however, such processes are rarely analyzed specifically for ventilated façade systems.

Given these gaps, experimental investigations under conditions representative of Kazakhstan's climatic regions are scientifically and practically justified. In addition, experimental studies will enable validation against the authors' previous research, which will further contribute to the development of climate-adapted recommendations for the design and operation of ventilated façades.

Thus, experimental research represents a key stage in establishing reliable heat and mass transfer models, ensuring the durability of building envelope structures, and improving building energy efficiency under high solar loads and hot-climate conditions.

2. METHODS AND MATERIALS

The methodology of the experimental study was based on a set of established rules and standards aimed at reproducing the operational, geometric, and structural parameters of real conditions. The

experimental program involved the use of appropriate test equipment, measuring instruments, and data acquisition systems, as well as modern software tools for data processing and analysis.

Since numerical simulations demonstrated a significant performance improvement of the proposed wall assembly due to the application of radiant barriers on the inner surfaces of alternating air channels, the following research tasks were defined prior to experimental testing:

- to develop a thermal insulation layer made of fibrous (mineral wool) insulation incorporating air channels and a radiant barrier;
- to construct a full-scale model of the adaptive wall system inside an experimental climatic chamber to reproduce the required thermal loading conditions, based on the most efficient configuration Scheme 3/50/75/50 identified in [27];
- to determine the thermophysical parameters of the adaptive wall assembly in the climatic chamber using a combined experimental-analytical approach in accordance with regulatory documentation, including thermal resistance (R-value), interlayer temperatures, and heat flux under both cold and hot operating periods;
- to evaluate, using experimental and analytical methods, the thermal resistance and heat flux through the investigated external wall envelope structure;
- to verify the agreement between the experimental results and the theoretical/numerical findings reported in the authors' previous study [27].

2.1 Description of the Adaptive Energy-Efficient External Wall System

A full-scale model of the developed adaptive external wall assembly was selected as the object of study. The model corresponds to the most efficient design configuration (Scheme 3/50/75/50) proposed in the authors' previous work [27]. The main design solutions and geometric parameters of the investigated envelope system are presented in Fig. 1 and Table 1.

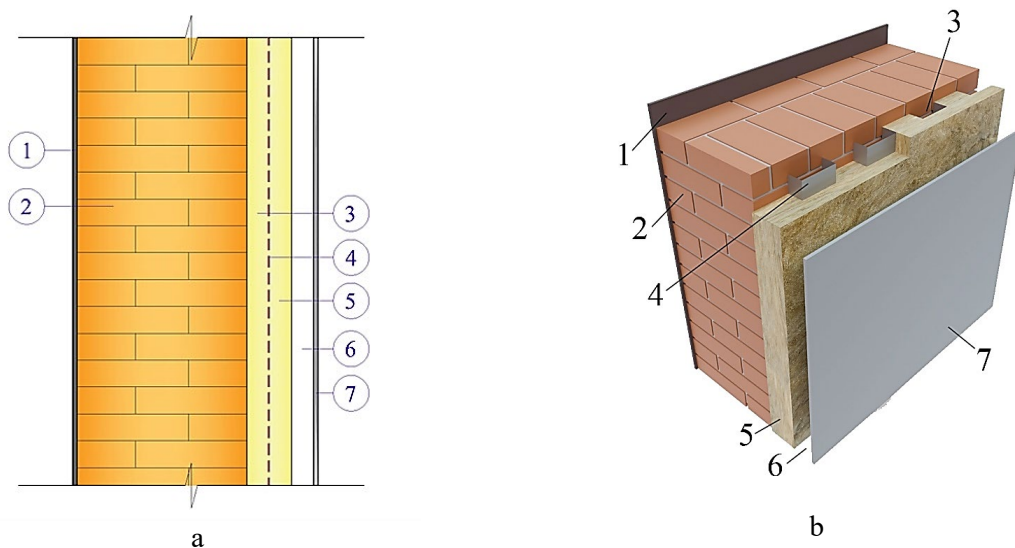


Fig. 1. Structural layout of the adaptive energy-efficient wall model: (a) side view; (b) general view. (1 – cement-sand plaster; 2 – ceramic brick masonry; 3 – air channel; 4 – radiant barrier; 5 – thermal insulation; 6 – air cavity; 7 – porcelain stoneware cladding).

Table 1. Layer characteristics of the new adaptive energy-efficient wall assembly [27].

Layer No.	Description	Thickness, mm	Width, mm	Thermal conductivity, λ (W/m \cdot °C)	Heat absorption coefficient, S (W/m 2 ·°C)	Vapor permeability, μ (mg/m \cdot h·Pa)	Emissivity of radiant barrier	
1	Cement-sand plaster	10	–	0.76	9.6	0.09	-	
2	Ceramic brick masonry	380	–	0.58	7.91	0.14	-	
4	Thermal insulation	Basalt mineral wool boards “DiRock Facade”, density 110 kg/m 3	75	–	0.035	0.3	0.005	0.039
5		Alternating vertical strips of basalt mineral wool / air	50	100	–	-	-	-
6	Air cavity	50	–	-	-	-	-	
7	Porcelain stoneware cladding	10	–	3.49	25.0	0.008	-	

A fragment of the developed insulation layer incorporating alternating air channels and a radiant barrier is shown in Fig. 2.

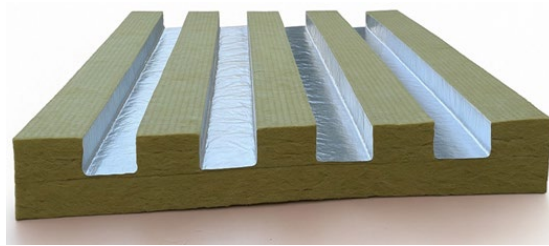


Fig. 2. Fragment of the insulation layer with alternating channels and a radiant barrier.

To meet the objectives of the experimental study, a full-scale wall fragment with dimensions of 3 m \times 3 m was installed in the climatic chamber. Thermal regimes were reproduced for the cold and hot periods [1]. The general view of the adaptive energy-efficient wall assembly prepared for climatic chamber testing is shown in Fig. 3.



a



b

Fig. 3. General view of the adaptive energy-efficient wall assembly prepared for climatic chamber testing: (a) cold-climate mode; (b) hot-climate mode.

2.2 Description of Experimental Instruments and Equipment

The thermal performance of the wall assembly under cold and hot operating conditions was investigated using a specialized climatic chamber. The chamber reproduced indoor (room) temperature conditions on one side GOST 30494-2011 and SP RK 2.04-107-2022, while on the opposite side it simulated negative temperatures corresponding to the cold period ($-14.3\text{ }^{\circ}\text{C}$, equal to the mean temperature of the coldest five-day period) and hot-period conditions ($+26.4\text{ }^{\circ}\text{C}$, equal to the mean outdoor air temperature in July) [1]. In the hot-period scenario, the thermal load was additionally simulated by heating both the cladding surface and the air using infrared lamps (Fig. 3b). The general layout of the climatic chamber is shown in Fig. 4.

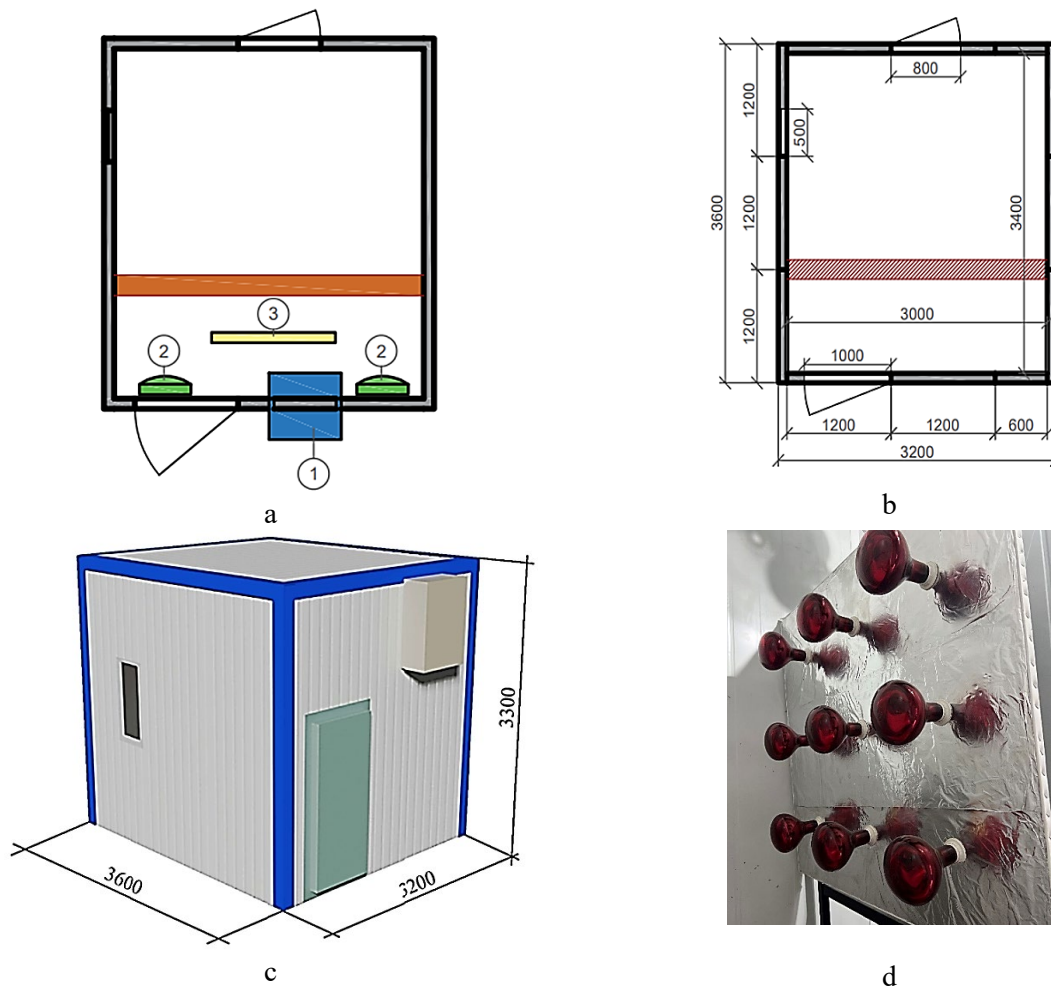


Fig. 4. Climatic chamber layout: (a) chamber plan (1 – air cooler, 2 – fan, 3 – solar radiation simulator); (b) structural scheme, mm; (c) general view of the climatic chamber, mm; (d) photograph of the solar radiation simulator.

Interlayer temperatures of the adaptive energy-efficient wall assembly were measured using DS18B20 five-channel temperature sensors with an operating range of $-55\text{ }^{\circ}\text{C}$ to $+125\text{ }^{\circ}\text{C}$. These sensors were integrated into a universal multi-channel temperature monitoring unit that enabled autonomous temperature recording and data storage on a memory card (Fig. 5). A dedicated software package was developed for data acquisition and processing of interlayer temperature values. The software ensured stable synchronization with Microsoft-based applications, facilitating data export and subsequent analysis (KZ11206).

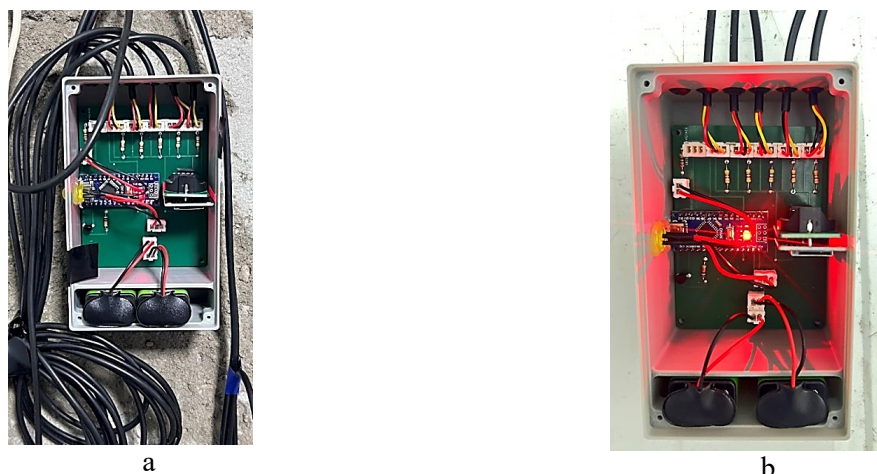


Fig. 5. Universal five-channel temperature measurement system: (a) general view; (b) during operation.

In parallel with the main measurements, thermal imaging was performed for both the cold and hot test periods to support validation. Thermograms were obtained using a Testo thermal imager with the IRSoft software for data analysis (Fig. 6a). Heat flux density was measured using the ITP MG-4.03 heat flux meter, designed for measuring and recording heat flux passing through single-layer and multilayer building envelope structures (Fig. 6b). The thermal resistance (R-value) of the investigated adaptive external wall assembly was determined using a combined experimental-analytical method in accordance with GOST 26254-84.



Fig. 6. Measuring instruments used in the experiments: (a) Testo thermal imager with analysis software; (b) ITP MG-4.03 heat flux density meter.

Measuring devices and primary transducers for temperature and heat flux were selected based on the expected ranges of test parameters under the prescribed temperature and humidity conditions in the climatic chamber and in accordance with the recommendations of GOST 25051.2-82.

The placement scheme of temperature sensors during climatic chamber testing on the wall fragment is presented in Fig. 7.

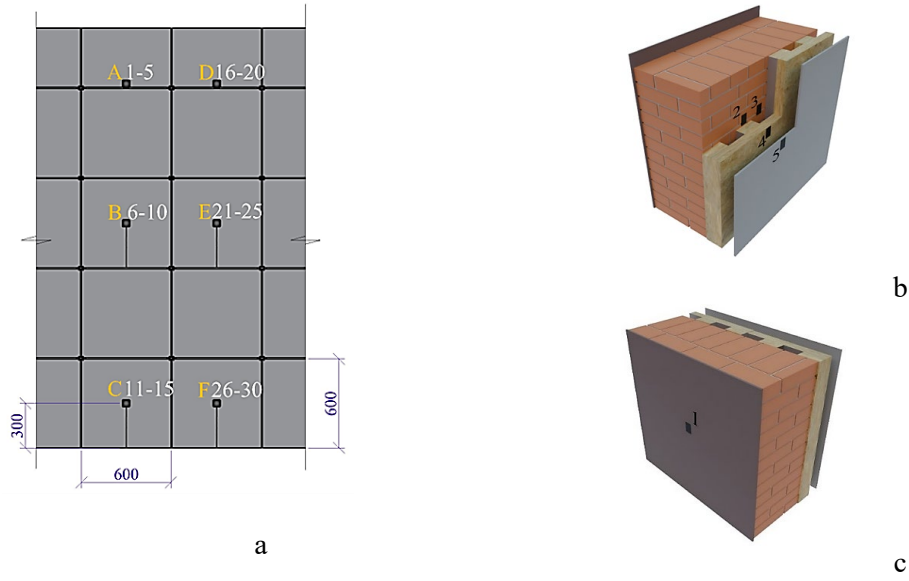
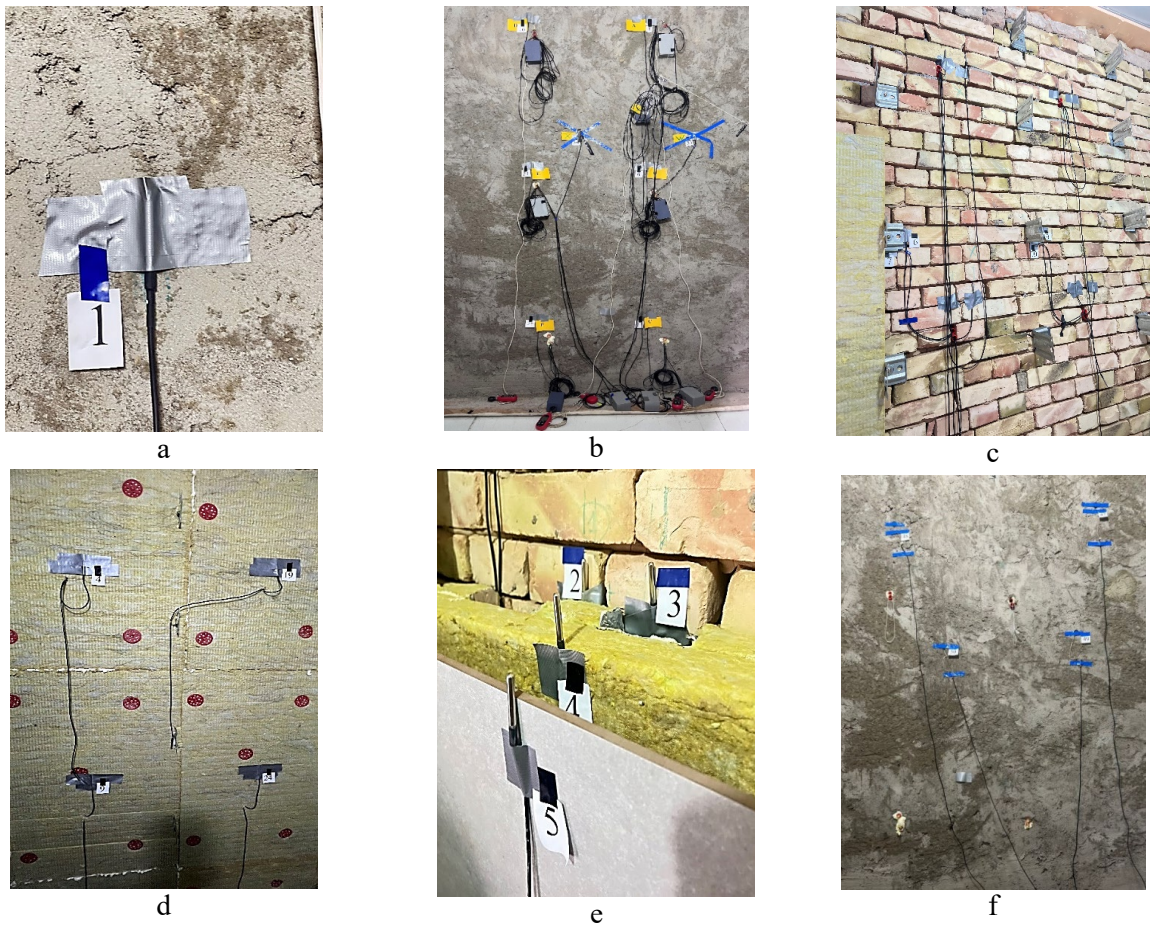


Fig. 7. Sensor layout during climatic chamber testing: (a) sensor installation scheme on the cladding, mm; (b, c) sensor installation scheme across envelope layers (numbering is provided in Table 4).

Photographs illustrating interlayer sensor placement during climatic chamber experiments are presented in Fig. 8.



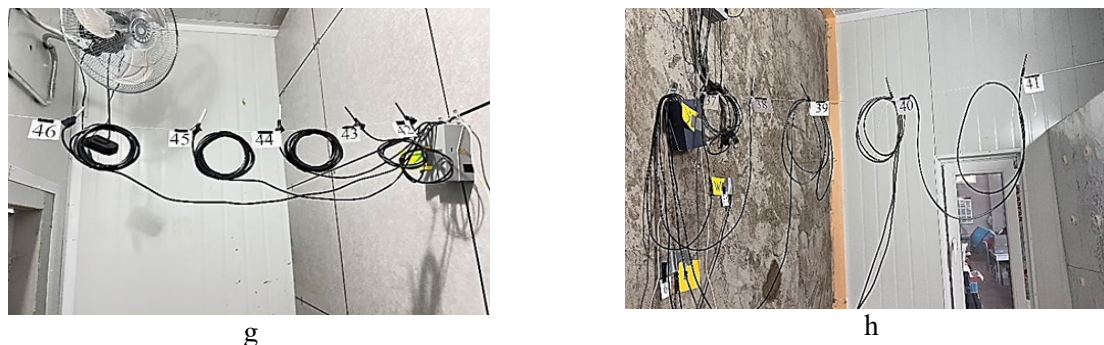


Fig. 8. Sensor placement during climatic chamber testing: (a) temperature sensor on the interior wall surface; (b) temperature sensors and data processing unit on the interior wall surface; (c) sensors between ceramic brick layers and the insulation layer, including the bracket zone; (d) sensors on the insulation surface; (e) sensors inside the air channel and on the cladding surface; (f) heat flux sensors on the interior wall surface; (g) sensors in the negative-temperature chamber; (h) sensors in the room-temperature chamber.

In accordance with the objectives of the experimental program, the tests evaluated interlayer temperatures, heat flux passing through the developed adaptive wall system, and thermal resistance under both cold and hot climatic conditions. Temperature and heat-flux sensors were fixed within the active zone exposed to negative and positive thermal loads. Sensor placement was designed to minimize measurement errors and to cover all vertical levels of the wall fragment installed in the climatic chamber.

2.3 Experimental Procedure for Assessing the Thermophysical Characteristics of the Adaptive Energy-Efficient Wall System

During the experimental study, the main thermophysical parameters of the proposed adaptive energy-efficient external wall assembly were measured. As noted in Section 2.1, the experiments were performed in a climatic chamber using a full-scale wall fragment under both cold and hot operating conditions. The key thermophysical and geometric characteristics of the investigated system, as well as the employed measuring instruments, are presented in the corresponding sections.

At the initial stage of testing, external and internal thermal loads were established by reproducing the required temperature conditions in the climatic chamber for the cold and hot scenarios. Subsequently, interlayer temperatures of the wall assembly were recorded. In addition, heat flux values were measured, and the thermal resistance (R-value) was determined using a combined experimental-analytical method in accordance with GOST 26254-84. All measured data were stored after signal processing by the data acquisition (secondary conversion) system.

The main workflow diagram of the experimental testing procedure for the new adaptive energy-efficient wall assembly in the climatic chamber, followed by validation against full-scale (field) investigation results, is presented in Fig. 9.

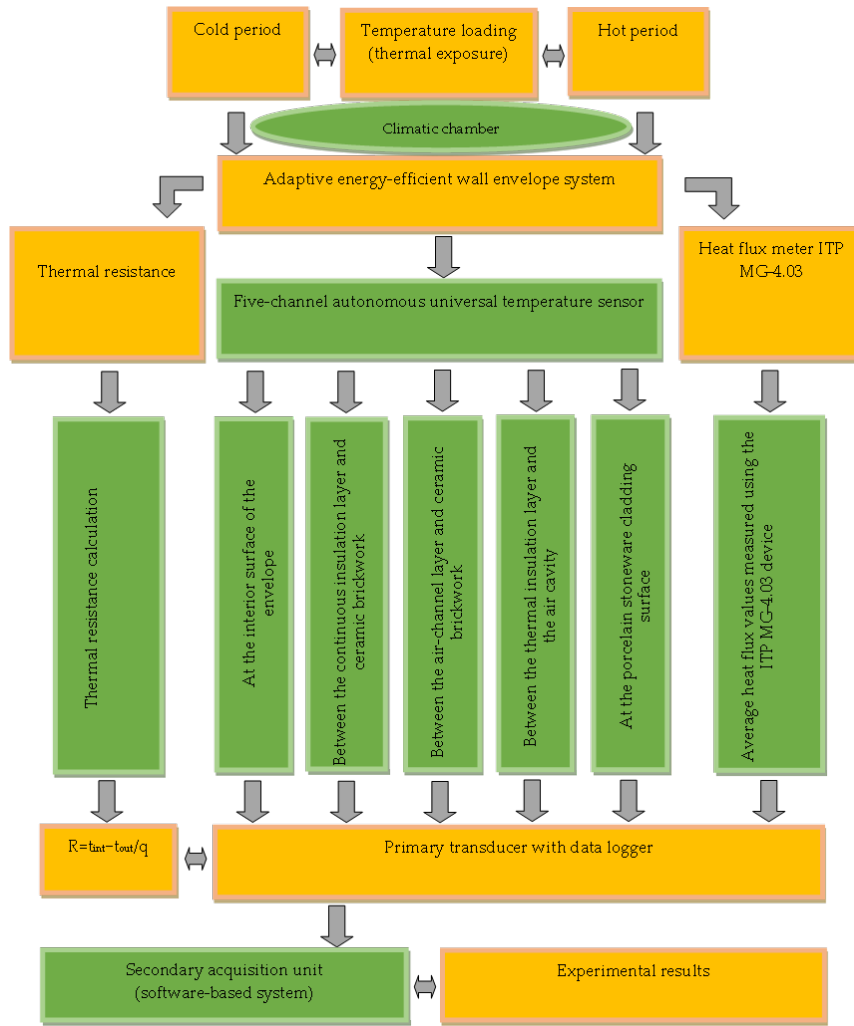


Fig. 9. Main experimental testing workflow (flowchart).

The main experimental test series for measuring the interlayer temperature values of the investigated wall assembly are summarized in Table 2.

Table 2. Experimental test series for interlayer temperature measurements.

Parameter	Cold period, °C (closed channels)	Hot period, °C (closed / ventilated channels)
Temperature conditions, °C	-14.3	+26.4
Test series	I	II-1/II-2
Temperature sensor labeling	Temperature sensor numbering	
A	1-5	1-5
B	6-10	6-10
C	11-15	11-15
D	16-20	16-20
E	21-25	21-25
F	26-30	26-30
Sensors located in the indoor (room-temperature) chamber		
Y (distance from the wall and spacing between sensors)	37(10 cm) 38(10 cm) 39(15 cm) 40(15 cm) 41(20 cm)	37(10 cm) 38(10 cm) 39(15 cm) 40(15 cm) 41(20 cm)

Continuation of Table 2

Sensors located in the cold chamber		
Z	42(10 cm)	42(10 cm)
(distance from the wall and	43(10 cm)	43(10 cm)
spacing between sensors)	44(15 cm)	44(15 cm)
	45(15 cm)	45(15 cm)
	46(20 cm)	46(20 cm)

During the hot-period test, the prescribed temperature represents the surface temperature of the cladding subjected to heating, as well as the air temperature in the chamber, as described in Section 2.1. Temperature sensors placed inside the indoor (room-temperature) compartment were used to measure the room temperature and validate the target temperature conditions maintained by the climatic chamber. A similar control measurement was performed in the cold compartment of the climatic chamber. The main experimental test series for measuring heat flux values through the investigated wall assembly are provided in Table 3.

Table 3. Experimental test series for heat flux measurements.

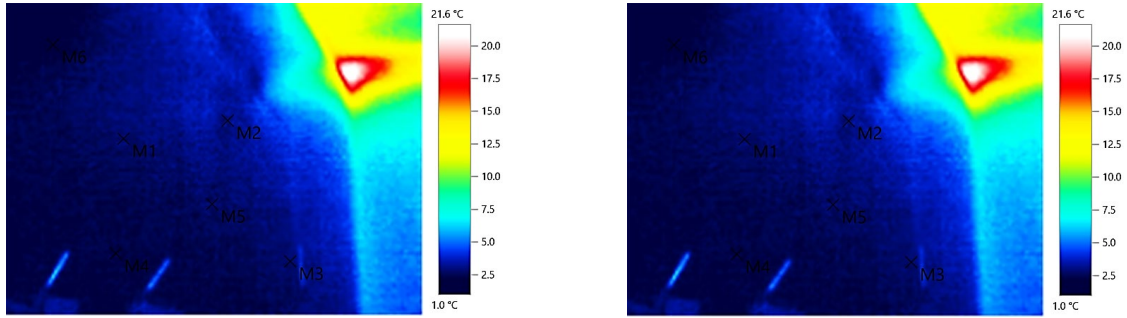
Parameter	Cold period, °C	Hot period, °C
Temperature conditions, °C	-14.3	+26.4
Sensor numbering	47-50	

In addition, both heat flux values and thermal resistance (R-value) were determined during experimental testing for the cold and hot scenarios.

3. RESULTS AND DISCUSSION

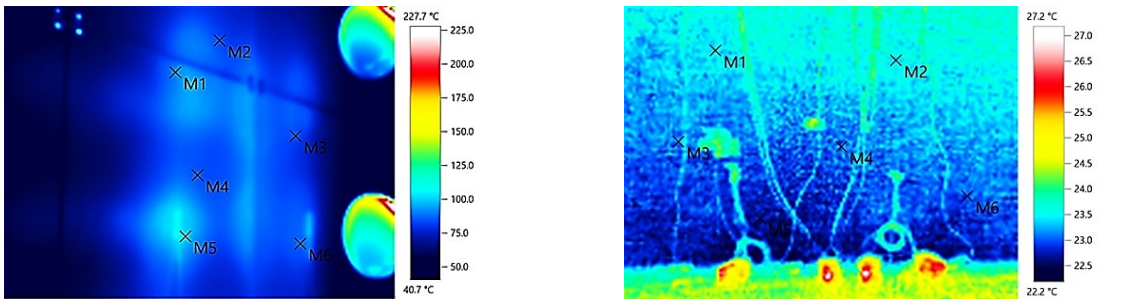
The experimental tests as a whole were carried out in two stages. The first stage corresponded to climatic chamber testing under cold-period conditions, where the range of temperature loads represented the environmental conditions, i.e., at -14.3 °C. At the second stage, the influence of hot climate conditions on the thermophysical parameters was examined, where the thermal load was simulated by heating the cladding of the investigated structure up to 46 °C [26] and by maintaining a constant room temperature simulating the environment at $+26.4$ °C. At the same time, in parallel, the heat flux passing through the proposed adaptive energy-efficient external wall envelope structure and the temperature values in the bracket zone were experimentally investigated. In addition, the thermal resistance of the specified structure was determined using a combined numerical-experimental method. The main block diagram and the experimental test series are presented in Fig. 9 and in Tables 2 and 3.

In accordance with the objectives of the study, at the first stage the interlayer temperature values of the proposed structure were determined under cold and hot climatic conditions. The reliability of the obtained temperature values on the internal and external surfaces of the envelope was additionally verified by thermal imaging (Fig. 10 and 11), the results of which showed consistency with the interlayer temperature values measured by the sensors (Table 4).



a. M1: -14.15°C; M2: -14.14°C; M3: -14.18°C; M4: -14.19°C; M5: -14.11°C; M6: -14.17°C. b. M1:19.54°C; M2:19.38°C; M3:19.33°C; M4:19.47°C; M5:19.34°C; M6:19.47°C.

Fig. 10. Thermograms of the cladding and the interior surface of the living room under cold-climate conditions at -14.3 °C: (a) cladding thermogram with characteristic temperature points; (b) thermogram of the interior room surface with characteristic surface points.



a. M1:46.11°C; M2:46.05°C; M3:46.15°C; M4:46.12°C; M5:46.01°C; M6:46.13°C. b. M1:24.35°C; M2:24.33°C; M3:24.40°C; M4:24.48°C; M5:24.31°C; M6:24.29°C.

Fig. 11. Thermograms of the cladding and the interior surface of the living room under hot-climate conditions at +26.4 °C (with cladding heating): (a) cladding thermogram with characteristic temperature points; (b) thermogram of the interior room surface with characteristic surface points.

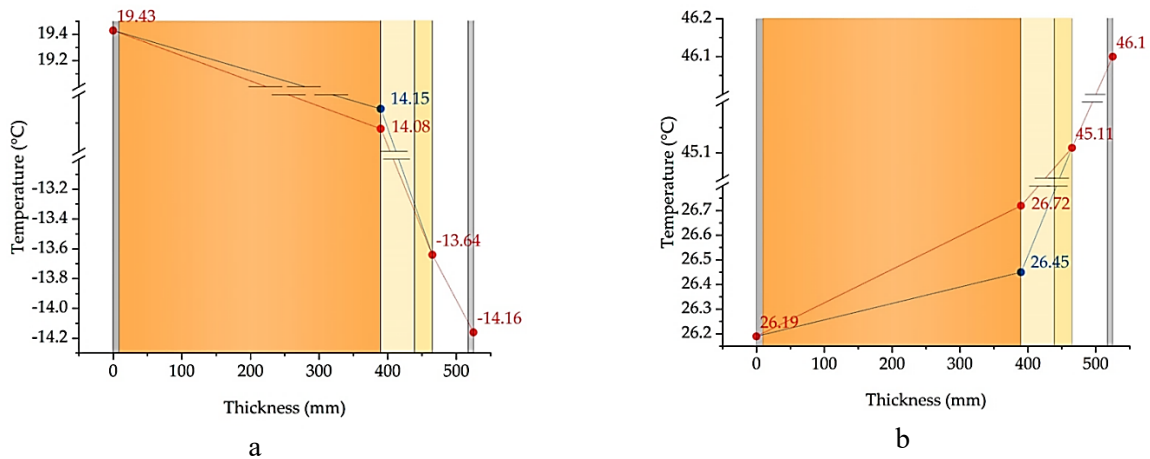
Table 4. Interlayer temperature values measured by the sensors.

Test series	Sensor label and temperature value	Installation location and sensor numbering (Figure 7)				
		1,6,11,16,21,26	2,7,12,17,22,27	3,8,13,18,23,28	4,9,14,19,24,29	5,10,15,20,25,30
Temperature values for each sensor with closed channels under cold-climate conditions						
I (-14.3°C)	A	No. 1	No. 2	No. 3	No. 4	No. 5
	t, °C	19.54	14.12	14.01	-13.61	-14.15
	B	No. 6	No. 7	No. 8	No. 9	No. 10
	t, °C	19.38	14.11	14.05	-13.64	-14.14
	C	No. 11	No. 12	No. 13	No. 14	No. 15
	t, °C	19.33	14.15	14.18	-13.62	-14.18
	D	No. 16	No. 17	No. 18	No. 19	No. 20
	t, °C	19.47	14.19	14.03	-13.64	-14.19
	E	No. 21	No. 22	No. 23	No. 24	No. 25
	t, °C	19.34	14.15	14.07	-13.66	-14.11
F	No. 26	No. 27	No. 28	No. 29	No. 30	
t, °C	19.47	14.13	14.09	-13.63	-14.17	

Continuation of Table 4

Temperature values for each sensor with closed channels under hot-climate conditions						
II-1 (+26.4°C)	A	No. 1	No. 2	No. 3	No. 4	No. 5
	t, °C	26.12	26.49	26.71	45.12	46.11
	B	No. 6	No. 7	No. 8	No. 9	No. 10
	t, °C	26.01	26.47	26.68	45.08	46.05
	C	No. 11	No. 12	No. 13	No. 14	No. 15
	t, °C	26.41	26.51	26.78	45.17	46.15
	D	No. 16	No. 17	No. 18	No. 19	No. 20
	t, °C	26.23	26.35	26.75	45.14	46.12
	E	No. 21	No. 22	No. 23	No. 24	No. 25
t, °C	26.12	26.35	26.61	44.99	46.01	
F	No. 26	No. 27	No. 28	No. 29	No. 30	
t, °C	26.25	26.49	26.77	45.15	46.13	
Temperature values for each sensor with ventilated channels under hot-climate conditions						
II-2 (+26.4°C)	A	No. 1	No. 2	No. 3	No. 4	No. 5
	t, °C	24.35	26.51	26.41	45.11	46.07
	B	No. 6	No. 7	No. 8	No. 9	No. 10
	t, °C	24.33	26.41	26.36	45.15	46.13
	C	No. 11	No. 12	No. 13	No. 14	No. 15
	t, °C	24.40	26.48	26.30	45.14	46.09
	D	No. 16	No. 17	No. 18	No. 19	No. 20
	t, °C	24.48	26.30	26.25	45.01	46.05
	E	No. 21	No. 22	No. 23	No. 24	No. 25
t, °C	24.31	26.32	26.28	45.21	46.18	
F	No. 26	No. 27	No. 28	No. 29	No. 30	
t, °C	24.29	26.44	26.32	45.28	46.23	

Based on the established overall interlayer temperature values of the developed envelope under different climatic conditions (cold and hot) and design configurations (closed and ventilated air channels within the insulation layer), averaged values were determined, which are presented in Fig. 12.



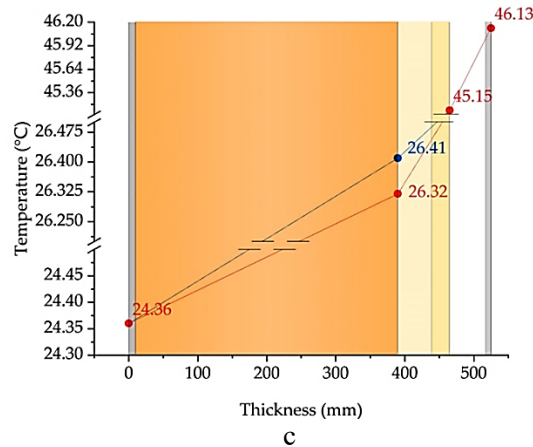


Fig. 12. Averaged interlayer temperature values under different climatic conditions (cold and hot): (a) temperature values for each sensor with closed channels under cold-climate conditions; (b) temperature values for each sensor with closed channels under hot-climate conditions; (c) temperature values for each sensor with ventilated channels under hot-climate conditions.

The analysis of the plots showed that the numerical studies [27] demonstrate sufficient agreement with the experimental data, confirming the effectiveness of the developed structure under both cold and hot climatic loads. At the same time, the reliability of the prescribed indoor temperature was monitored using additional temperature sensors (Fig. 8g, h), which also showed consistency with the target temperature values maintained by the climatic chamber (Table 5), indicating high quality of the obtained results.

Table 5. Temperature values in the chamber, where Y denotes temperature sensors installed in the indoor (room-temperature) chamber, and Z denotes temperature sensors installed in the outdoor chamber simulating the ambient environment.

Sensor label and installation location		Sensor number and temperature value of each sensor and its position (distance from the wall and spacing between sensors)					Mean, °C
Test series	Y	10 cm	10 cm	15 cm	15 cm	20 cm	
			No. 37	No. 38	No. 39	No. 40	No. 41
I (-14.30°C)	Y	20.55	20.68	20.72	20.75	20.75	20.69
II-1 (26.40°C)		26.05	25.71	25.32	24.54	24.01	25.13
II-2 (26.40°C)		25.41	25.35	25.22	24.12	23.85	24.79
Test series	Z	No. 42	No. 43	No. 44	No. 45	No. 46	
I (-14.30°C)		-14.25	-14.39	-14.30	-14.31	-14.31	-14.32
II-1 (26.40°C)		26.38	26.39	26.40	26.41	26.41	26.40
II-2 (26.40°C)		24.38	24.11	24.02	23.98	23.95	24.09

According to the methodology presented in Fig. 9, the heat flux values for cold and hot climatic conditions were determined and are presented in Fig. 13.

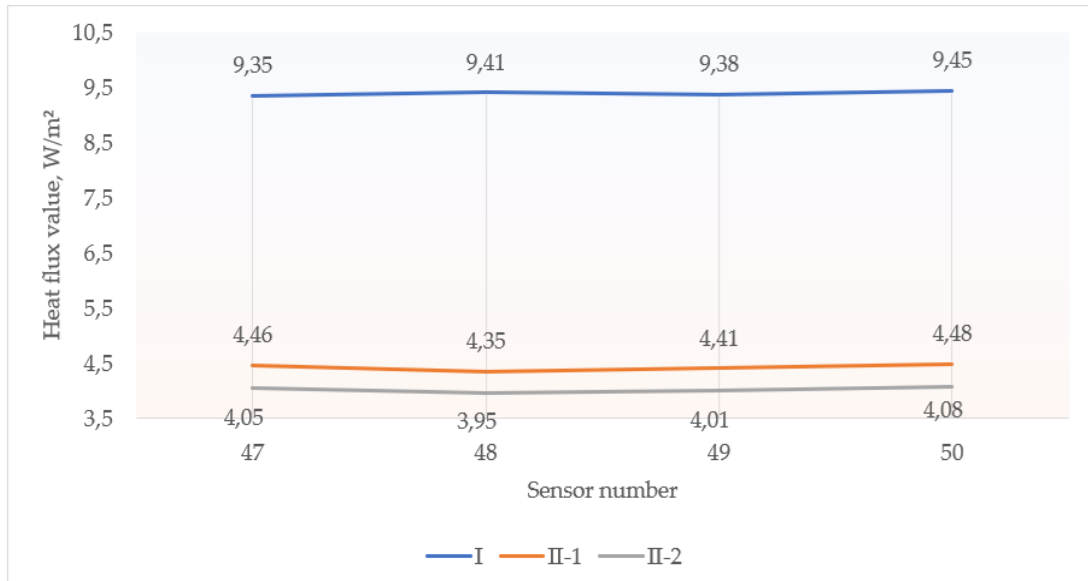


Fig. 13. Heat flux values for the cold and hot periods (Fig. 8f).

The obtained heat flux density values also indicate satisfactory agreement with the authors’ numerical studies [27]. In addition, in the present study the authors further evaluated the temperature values in the zone of steel brackets; these values were also determined and summarized in Table 6.

Table 6. Temperature values in the bracket zone for the cold and hot periods (Fig. 8c). Values without a prime correspond to temperature sensors positioned horizontally, whereas prime-marked values correspond to sensors positioned vertically.

Test series	Bracket number and temperature value, °C					
	VI-1		VI-2		VI-3	
I (-14.30°C)	9.81	9.98′	10.05	9.95′	9.07	9.91′
II-1 (26.40°C)	27.01	26.98′	27.00	26.95′	27.05	26.93′
II-2 (26.40°C)	26.41	26.48′	26.40	26.412	26.45	26.48′

The performed analysis of temperature values in the bracket zone makes it possible to quantitatively assess the thermal bridge effect. The comparison confirmed that, despite their presence (brackets), the overall thermal resistance of the structure remains within the regulatory requirements, which is also consistent with the assumptions adopted in the modeling.

The interlayer temperature values of the adaptive envelope and the heat flux values established above contributed to determining the thermal resistance of the developed adaptive envelope for cold and hot climates SP RK 2.04-107-2022, (Fig. 14).

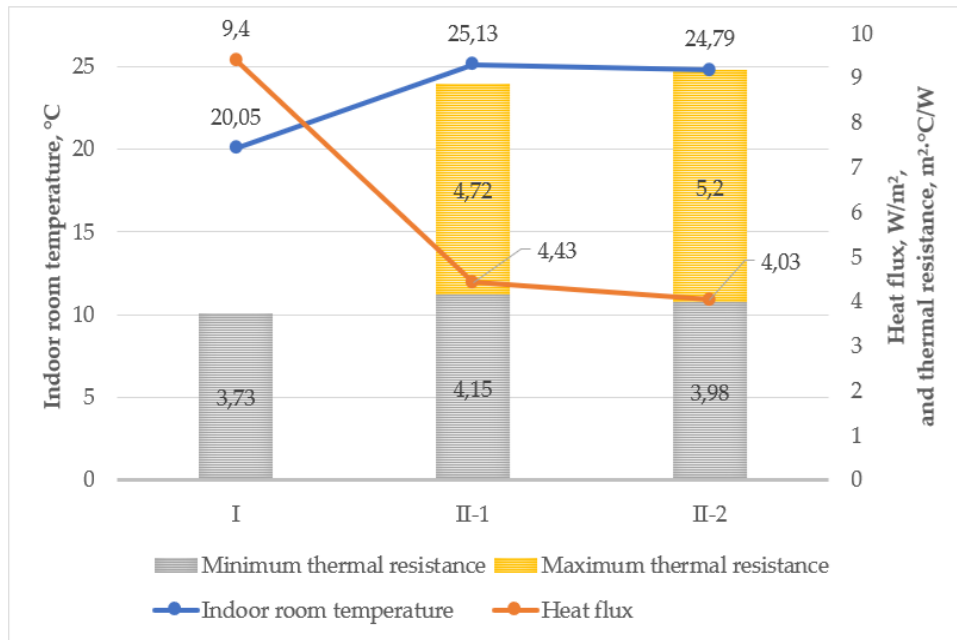


Fig. 14. Thermal resistance values as a function of the test series for the cold and hot periods.

The thermal resistance values obtained during the experimental studies also showed agreement with the values established in the modeling of the developed envelope, which serves as the final confirmation of the energy efficiency of the structure.

The conducted experimental tests confirm the high efficiency of the structure and the reliability of the thermophysical values determined in the modeling of the developed adaptive structure under different temperature loads [27], where the most important results were obtained in the hot-climate simulation mode. In this mode, the structure demonstrated the ability to adapt by switching the air cavity to the ventilation mode, which was confirmed by a sharp decrease in heat flux density. The parallel investigation of thermal bridges confirmed that, despite their presence (brackets), the overall thermal resistance of the structure remains within the regulatory requirements, which is also consistent with the assumptions adopted in the modeling. Thus, this work translates the results of the numerical study [27] into the domain of an empirically proven, implementation-ready technology.

The obtained results demonstrate high consistency with the heat and mass transfer patterns established in international studies on adaptive façade systems. A systematic review [28] shows that the use of façades with a controllable air channel can reduce annual building energy consumption by approximately 15%, which lies within the same range as the effect identified in the present study. As noted in [17], the geometric parameters of the air cavity have a critical influence on the development of natural convection and the thermal response of envelope structures; this statement is fully confirmed by the obtained data, according to which reducing the thickness of the air layer from 100 to 50 mm leads to a noticeable increase in the thermal efficiency of the system. The results of [29] also confirm the importance of intensifying ventilation of the air gap, demonstrating a reduction in the external surface temperature by 3-5 °C, which correlates with the experimental values recorded in this study. Similar conclusions are reported in [29], emphasizing that the maximum efficiency of adaptive façades is achieved in climates with high solar radiation intensity – such as the climate of the southern regions of Kazakhstan [30].

Nevertheless, the study has a number of limitations inherent to the experimental-numerical approach. The model did not account for wind gusts with speeds above 6 m/s, which can potentially reorganize airflow patterns inside the channel and enhance convective heat transfer. Solar radiation effects were simulated without considering variable cloudiness, reflected radiation, and local shading, which may result in underestimation of short-term fluctuations in thermal load. In addition, aerodynamic processes typical of the upper zones of high-rise buildings were not considered, where

vortex formations and unstable convective regimes may occur. These factors may become the subject of further research.

Taking into account the indicated limitations, the results have significant practical value. The adaptive composite façade scheme demonstrates the ability to reduce heat losses in the winter period by up to 18% and summer heat gains by up to 14%, which provides a tangible reduction in operating costs. Due to the modularity of the structure and the absence of the need for complex engineering systems, the adaptive façade can be effectively applied both in new construction and in modernization projects for buildings with a height of 5-25 storeys. This makes the proposed technology a promising solution for the climatic conditions of Central Asian countries.

An important outcome is that the experimental data confirmed the correctness of previously obtained model predictions. This demonstrates the reliability of the methodological approach and also confirms the high energy-efficiency potential of the developed structure under the hot climatic conditions of Kazakhstan (KZ11495, KZ36701.).

4. CONCLUSIONS

Based on the experimental testing of a full-scale model of the adaptive composite energy-efficient wall structure in a climatic chamber, key conclusions were formulated, confirming both the scientific validity and the practical relevance of the developed solution. It was experimentally established that the Scheme 3/50/75/50 structure fully validates the results of the previously performed numerical modeling, demonstrating optimal thermophysical characteristics under both low and high temperature impacts. The determined reduced thermal resistance confirmed the high energy efficiency of the system, showing its ability to meet and even exceed regulatory requirements under various climatic regimes. Quantitative measurements of heat flux density and temperature gradients also demonstrated the operability of the adaptive mechanism based on alternating air channels and the use of a radiant barrier, which ensures a significant reduction in heat gains under conditions of intense solar radiation due to the transition of the structure to the natural ventilation mode. Taking into account the identified limitations of the study, the obtained results nevertheless have high practical value: the adaptive façade scheme demonstrates the ability to reduce heat losses in the winter period by up to 18% and summer heat gains by up to 14%, which leads to lower operating costs and improved overall building energy efficiency. Due to the modularity of the structure, ease of integration, and the absence of the need for complex engineering systems, the developed façade can be effectively applied both in new construction and in modernization of buildings with heights of 5-25 storeys. This makes the presented technology a promising solution for the climatic conditions of Central Asian countries and provides a scientific and technical basis for further development of design standards for adaptive façade systems.

5. ACKNOWLEDGEMENTS

This research is funded by the Science Committee of the Ministry of Science and Higher Education of the Republic of Kazakhstan (Grant No. AP22782896)

As a result of the work, we obtained two patents for utility model of the Republic of Kazakhstan «Mobile universal complex for measuring the thermophysical parameters of external building envelopes», 2025, No. 11206; «Adaptive energy-efficient exterior wall construction», 2025, No. 11495 and one patent for invention of the Republic of Kazakhstan «Energy-saving wall enclosing structure with air channels», 2024, No. 36701.

REFERENCES

1. Zhangabay N., Giyasov A., Ibraimova U., Tursunkululy T., Kolesnikov A. Construction and climatic certification of an area as a prerequisite for development of energy-efficient buildings and their external wall constructions. *Construction Materials and Products*. 2024. 7 (5). P. 1. DOI:<https://doi.org/10.58224/2618-7183-2024-7-5-1>
2. Jankovic A. and Goia F. Impact of double skin facade constructional features on heat transfer and fluid dynamic behaviour. *Building and Environment*. 2021. 196. P. 107796. DOI: <https://doi.org/10.1016/j.buildenv.2021.107796>
3. Ibrahim R.A., Imghoure O., Tittlein P., Belouaggadia N., Chehade F.H., Sebaibi N., Stéphane L., Zalewski L. Application of Ventilated Solar Façades to enhance the energy efficiency of buildings: A comprehensive review. *Energy Reports*. 2025. 13. P. 1266 – 1292. DOI: <https://doi.org/10.1016/j.egy.2024.12.051>
4. Zhangabay N., Tagybayev A., Utelbayeva A., Baganova S., Tolganbayev A., Tulesheva G., Jumabayev A., Kolesnikov A., Kambarov M., Imanaliyev K., Kozlov P. Analysis of the influence of thermal insulation material on the thermal resistance of new facade structures with horizontal air channels. *Case Studies in Construction Materials*. 2023. 18. P. e02026. <https://doi.org/10.1016/j.cscm.2023.e02026>
5. Zhangabay N., Tagybayev A., Baidilla I., Sapargaliyeva B., Shakeshev B., Baibolov K., Duissenbekov B., Utelbayeva A., Kolesnikov A., Izbassar A. Multilayer External Enclosing Wall Structures with Air Gaps or Channels. *J. Compos. Sci*. 2023. 7. P. 195. DOI: <https://doi.org/10.3390/jcs7050195>
6. Borodulin V.Yu., Nizovtsev M.I. Modeling heat and moisture transfer of building facades thermally insulated by the panels with ventilated channels. *Journal of Building Engineering*. 2021. 40. P. 102391. DOI: <https://doi.org/10.1016/j.job.2021.102391>
7. Nizovtsev M.I., Letushko V.N., Borodulin V.Yu., Sterlyagov A.N. Experimental studies of the thermo and humidity state of a new building facade insulation system based on panels with ventilated channels. *Energy and Buildings*. 2020. 206. P. 109607. DOI: <https://doi.org/10.1016/j.enbuild.2019.109607>
8. Nizovtsev M.I., Borodulin V.Yu. Calculation of the Efficiency of Regenerative Air Heat Exchanger with Intermediate Heat Carrier. *Journal of Construction Research*. 2021. 2. P. 30 – 36. DOI: <https://doi.org/10.30564/jcr.v3i1.3235>
9. Statsenko E.A., Ostrovaia A.F., Olshevskiy V.Y., Petrichenko M.R. Temperature and velocity conditions in vertical channel of ventilated facade. *Magazine of Civil Engineering*. 2018. 80(4). P. 119 – 127. DOI: <https://doi.org/10.18720/MCE.80.11>
10. Jha P.B. Impact of temperature dependent heat source on MHD natural convection flow between two vertical plates filled with nanofluid with induced magnetic field effect. *Arab Journal of Basic and Applied Sciences*. 2020. 1. P. 299 – 312. <https://doi.org/10.1080/25765299.2020.1806484>
11. Rahiminejad M., Khovalyg D. Experimental study of the hydrodynamic and thermal performances of ventilated wall structures. *Building and Environment*. 2023. 233. 1. P. 110114. DOI: <https://doi.org/10.1016/j.buildenv.2023.110114>
12. Yuan J. Impact of Insulation Type and Thickness on the Dynamic Thermal Characteristics of an External Wall Structure. *Sustainability*. 2018. 10. 2835. <https://doi.org/10.3390/su10082835>
13. Özturan M.K., Seyhan K. Determination of optimum insulation thickness of building walls according to four main directions by accounting for solar radiation: A case study of Erzincan, Türkiye. *Energy and Buildings*. 2024. 304. P. 113871. DOI: <https://doi.org/10.1016/j.enbuild.2023.113871>
14. Shahid M., Karimi M.N., Mishra A.K. Optimum insulation thickness for external building walls for different climate zone in India. *Journal of Thermal Engineering*. 2024. 10 (5). P. 1198 – 1211. <https://izlik.org/JA93UH79KL>

15. Uçar A. Optimization of insulation thickness of walls and roofs using energy, exergy, economic and environmental analyses. 2024. 18. P. 9959 – 9975. DOI: <https://doi.org/10.15282/jmes.18.1.2024.12.0787>
16. Aggarwal C., Molleti S. State-of-the-Art Review: Effects of Using Cool Building Cladding Materials on Roofs. *Buildings* 2024, 14, 2257. <https://doi.org/10.3390/buildings14082257>
17. Vasileva I.L., Nemova D.V., Vatin N.I., Fediuk R.S. & Karelina, M.I. Climate-Adaptive Façades with an Air Chamber. *Buildings*. 2022. 12. P. 366. DOI: <https://doi.org/10.3390/buildings12030366>
18. Cuce P.M., Cuce E. Ventilated Facades for Low-Carbon Buildings: A Review. *Processes*. 2025. 13. P. 2275. DOI: <https://doi.org/10.3390/pr13072275>
19. Lin Z., Song Y., Chu Y. An experimental study of the summer and winter thermal performance of an opaque ventilated facade in a cold zone of China. *Building and Environment*. 2022. P. 109108. DOI: <https://doi.org/10.1016/j.buildenv.2022.109108>
20. Zhangabay N., Tursunkululy T., Utelbayeva A., Abdikerova U., Sultanov M. A Study of Temperature and Humidity Conditions in a New Energy-Efficient Design of a Wall Structure with Air Gaps. *Modelling*. 2025. 6. P. 12. DOI: <https://doi.org/10.3390/modelling6010012>
21. Zhangabay N., Bonopera M., Baidilla I., Utelbayeva A., Tursunkululy T. Research of Heat Tolerance and Moisture Conditions of New Worked-Out Face Structures with Complete Gap Spacings. *Buildings*. 2023. 13. P. 2853. DOI: <https://doi.org/10.3390/buildings13112853>
22. Zhangabay N., Oner A., Rakhimov M., Tursunkululy T., Abdikerova U. Thermal Performance Evaluation of a Retrofitted Building with Adaptive Composite Energy-Saving Facade Systems. *Energies* 2025. 18. P. 1402. DOI: <https://doi.org/10.3390/en18061402>
23. Duissenbekov, B., Tokmuratov, A., Yerimbetov, B., Aldiyarov, Z. Finite-difference equations of quasistatic motion of the shallow concrete shells in nonlinear setting. *Curved and Layered Structures*, 2020. 7 (1). P. 48 – 55. <https://doi.org/10.1515/cls-2020-0005>
24. Grillo E., Sansotta S. Experimentation of a new adaptive model for envelope system. In: Sposito, C. (ed.) *Possible and preferable scenarios of a sustainable future*. 2021. DOI: <https://doi.org/10.19229/978-88-5509-232-6/5102021>
25. Fohagui F., Koholé Y., Alombah N., Asoh D., Tchuen G. Optimum insulation thickness and exergy savings of building walls in Bamenda: a comparative analysis. *Energy Storage and Saving*. 2024. 3. P. 60 – 70. <https://doi.org/10.1016/j.enss.2024.01.001>
26. Mishra S., Kalla S., Agarwal Y., Gupta V. Parametric analysis of energy saving in building walls by applying various insulation materials. *Journal of Polymer and Composites*. 2024. 11(12). P. 113 – 118. <https://journals.stmjournals.com/jopc/article=2024/view=131314> (accessed on 20.08.2025)
27. Zhangabay N., Oner A., Ibrahimova U., Ibrahim M.N.M., Tursunkululy T., Utelbayeva A. Assessment and Numerical Modeling of the Thermophysical Efficiency of Newly Developed Adaptive Building Envelopes Under Variable Climatic Impacts. *Buildings* 2026. 16. P. 366. DOI: <https://doi.org/10.3390/buildings16020366>
28. Andreeva D., Nemova D., Kotov E. Multi-Skin Adaptive Ventilated Facade: A Review. *Energies* 2022. 15. P. 3447. DOI: <https://doi.org/10.3390/en15093447>
29. Schabowicz K., Zawisłak Ł., Staniów P. Efficiency of ventilated facades in terms of airflow in the air gap. *Studia Geotechnica et Mechanica*, 2021. 43(3). P. 224 – 236. DOI: <https://doi.org/10.2478/sgem-2021-0014>
30. Pujadas-Gispert E., Alsailani, K.C.A. van Dijk A.D.K. Rozema J.P. ten Hoope C.C. Korevaar S.P.G. Moonen (Faas). Design, construction, and thermal performance evaluation of an innovative bio-based ventilated façade. *Frontiers of Architectural Research*. 2020. 9 (3). P. 681 – 696. DOI: <https://doi.org/10.1016/j.foar.2020.02.003>

INFORMATION ABOUT THE AUTHORS

Zhangabay N.Zh., e-mail: Nurlan.Zhanabay777@mail.ru, ORCID: <https://orcid.org/0000-0002-8153-1449>, SCOPUS: <https://www.scopus.com/authid/detail.uri?authorId=57211557292>, South-Kazakhstan University named after M. Auezov, Department «Architecture and urban planning», Candidate of Engineering sciences (PhD), Associate Professor

Oner A.K., e-mail: arukhanoner@mail.ru, ORCID: <https://orcid.org/0009-0001-6230-0645>, SCOPUS: <https://www.scopus.com/authid/detail.uri?authorId=59710483600>, Abylkas Saginov Karaganda Technical University, Department of Building Materials and Technologies, Doctoral Student

Ibrahim M.N.M., e-mail: mnm@usm.my, ORCID: <https://orcid.org/0000-0002-6784-5775>, SCOPUS: <https://www.scopus.com/authid/detail.uri?authorId=55909512200>, Materials Technology Research Group (MaTRec), School of Chemical Sciences, Universiti Sains Malaysia, Doctor, Professor

Ibraimova U.B., e-mail: ibraimova_uljan@mail.ru, ORCID: <https://orcid.org/0009-0004-9786-1348>, SCOPUS: <https://www.scopus.com/authid/detail.uri?authorId=58368006200>, M. Auezov South Kazakhstan University, Department of Architecture and urban planning, Candidate of Engineering Sciences (Ph.D.)

Kolesnikov A.S., e-mail: kas164@yandex.kz, ORCID: <https://orcid.org/0000-0002-8060-6234>, SCOPUS: <https://www.scopus.com/authid/detail.uri?authorId=57189499212>, South-Kazakhstan University named after M. Auezov, Department of Life safety and environmental protection, Candidate of Technical Sciences (PhD), Professor

Tursunkululy T., e-mail: timurtursunkululy@gmail.com, ORCID: <https://orcid.org/0000-0001-6215-7677>, SCOPUS: <https://www.scopus.com/authid/detail.uri?authorId=57687675500>, South-Kazakhstan University named after M. Auezov, Department «Architecture and urban planning», Candidate of Engineering Sciences (Ph.D.)